터널과 지하공간, 한국암반공학회지
제14권 제6호, 2004년 12월, pp. 411~422

TUNNEL & UNDERGROUND SPACE, Vol. 14, No. 6, 2004, pp. 411-422
Journal of Korean Society for Rock Mechanics

Analysis of Sinkhole Formation over Abandoned Mine using Active-Passive-Active Finite Elements

Debasis Deb[1], Sung O. Choi[2]* and Hee-Soon Shin[3]

폐광지역에서의 싱크홀 발생 규명을 위한 Active-Passive-Active 유한요소 기법 연구

Debasis Deb, 최성웅, 신희순

Abstract Sinkhole subsidence occurs over abandoned mine workings and can be detrimental to human lives, damage to properties and other surface structures. In this study, simulation of sinkhole development process is performed using special finite element procedure. Especially, creation of mine voids due to roof falls and generation of goaf from broken rocks are simulated using active-passive-active finite elements. An active or solid element can be made passive or void once the tensile failure criterion is satisfied in the specified sinkhole formation zone. Upon completion of sinkhole development process, these passive elements can again be made active to simulate goaf region. Several finite element models are analyzed to evaluate the relationships between sinkhole formation with width of gallery, depth of mine, roof condition and bulking factor of roof rocks. This study demonstrates that the concept of passive elements in numerical analysis can be used effectively for analyzing sinkhole formation or roof fall phenomenon in general.

KeyWords sinkhole, abandoned mine, active-passive-active finite element, bulking factor

초 록 폐광지역에서 흔히 발생하는 싱크홀 형태의 지반침하는 인근 지역 주민의 안전은 물론, 지상구조물에 심각한 위해 요소로 작용할 수 있다. 본 연구에서는, 이러한 싱크홀의 발생양상을 수치해석적으로 규명하기 위해, 아주 특별한 형태의 유한요소해석을 실시하였다. 특히, 갱도 천반의 붕락에 의해 야기되는 공간이나, 파쇄된 암반이 쌓여서 이루는 폐석더미 등 기존의 수치해석기법으로서는 쉽사리 표현할 수 없었던 현실적인 문제들을 수치적으로 모사하기 위해 active-passive-active 유한요소를 사용하였다. Active 요소 즉 고체 요소는 싱크홀이 형성되는 영역 내에서 인장파괴 기준식을 만족하게 되면 passive 요소 즉 공간 요소로 전환될 수 있다. 싱크홀이 완전히 형성되게 되면 이들 passive 요소들은 다시 active 요소로 바뀌면서 폐석더미를 수치적으로 모사할 수 있게 된다. 채굴적의 폭, 심도, 천반의 상태 및 붕락 암반의 부피팽창율 등이 싱크홀에 미치는 영향을 검토하기 위해 여러 가지 조건에 의한 유한요소모델이 해석되었다. 본 연구는, 이와 같이 싱크홀이 발생하는 과정이나 천반이 붕락하는 현상 등을 해석하기 위해 수치해석상에서 active-passive-active 유한요소들이 효과적으로 사용될 수 있음을 보여준다.

핵심어 싱크홀, 폐광지역, active-passive-active 유한요소, 부피팽창율

1. Introduction

Abandoned mine workings exist in many countries including Korea and sometimes the extent of working may not be known. Most of the old mines are worked with room and pillar method of mining and possesses great potential of surface subsidence by roof fall/ pillar failure. In UK, more than 70,000 old mine workings are reported and some of them may be three centuries old (Whittaker & Reddish, 1989). In the USA, 354 subsidence incidents were reported over the Pittsburgh Coal bed most of which in the form

[1] 한국지질자원연구원 지반안전연구부 Postdoctoral Research Fellow
[2] 한국지질자원연구원 지반안전연구부 선임연구원
[3] 한국지질자원연구원 지반안전연구부장 책임연구원
*교신저자(Corresponding Author): choiso@kigam.re.kr
접수일: 2004년 12월 1일
심사 완료일: 2004년 12월 23일

of sinkholes (Gray *et al.*, 1977). In 1985, Marino et al. reported that both trough and sinkhole type subsidence occurred in Illinois (Whittaker *et al.*, 1989) over shallow depth room and pillar mines. After extensive study of surface subsidence in the USA, Gray *et al.* commented that the most prevalent subsidence features over abandoned mined land are sinkholes, with depth of sinkhole more than 3 ft, and trough or sags less than 3 ft (Peng, 1992). After studying subsidence incidents in Germany, Kratzsch commented that sudden cave-ins and irregular depressions in the form of sinkholes over near-surface abandoned mines possess a serious risk to the populated area nearby (Kratzsch, 1985). His study also suggests that size of the effected area must be established based on statistical investigations, taking into account the type of workings, strength and thickness of roof, fluctuation of ground water and others. In Korea, more than 300 coal mines have been ceased of their operations with the economic structural adjustments in early 1990s. With lots of abandoned coal mines, the surface subsidence problem has been coming up to the public, known as one of geohazards (Choi *et al.*, 2004). Their study suggests that several parameters should be emphasized for evaluating the surface subsidence in coal mine area, and these parameters should be dealt with adding an extra weight for realistic analysis. In addition, the sinkhole type subsidence in urban area, whatever it caused by gangway collapse in coal mines or in metal mines, can be a death-blow to many structures as well as public welfare. The surface subsidence in the Boopyung graveyard was one example for this. It happened by the roof fall and pillar failure in near-surface openings and was restored by pumping the sand slurry into those openings (KIGAM report, 1993).

All of the above mentioned literatures suggest that sinkhole development is a process of collapsed junction having a weak/fractured roof and then progression of chimney collapse up to the surface at shallow depth of cover. In general, sinkhole is in the form of conical depression/cavity suddenly appears on the surface. The major factors which contribute to sinkhole formation are width of mine opening/gallery (w), height of opening (M), depth of cover (H), rock type and thickness of roof, water condition, pillar strength, time elapsed after mining operation was ceased, inclination of the seam, bulking factor (K) of roof rocks and others. Whittaker *et al.* (1989) reported that width of gallery, depth of cover and roof conditions are the primary factors for the determination of sinkhole occurrences and higher chances are associated with lower H, higher w and weak roof conditions. Peng (1992) had also commented on the similar factors which contributed to sinkhole development in the Pittsburgh Coal bed.

Simulation of sinkhole development process is complex and general purpose numerical software packages cannot effectively be used to analyze the roof breakage phenomenon incorporating bulking effect of broken rocks. Thus, in this study, a special algorithm is developed to systematically simulate roof breakage phenomenon and goaf formation using active-passive-active finite elements. An active element is synonymous to a solid area in the model. Passive element is introduced to represent excavation area or to generate cavity area caused by roof falls so that successive roof breakage phenomena can be simulated. It is a similar approach adopted for simulating excavation sequence of underground mining (Najjar & Zaman, 1993) except in this case, the elements are declared passive or excavated based on tensile failure criterion as opposed to manual sequencing technique. Another advantage of this technique is that the passive elements can again be made active to simulate goaf region once the volume occupied by the broken rocks equals to the void volume or sinkhole appears on the surface. This paper provides details of the finite element formulation with passive elements. This study is also extended to analyze sixteen different models by varying width of the gallery, depth of mine void, roof conditions and bulking factor of roof rocks.

Rock mass outside the sinkhole formation zone is analyzed based on elastic-plastic material properties with generalized Hoek and Brown failure criterion. This paper also provides detail procedure of this technique for finite element formulation.

2. Volumetric calculations of sinkhole formation

In this study, sinkhole is assumed to be cylindrical shape all through its length. Considering the diameter of the chimney or sinkhole as D, the height of collapsed chimney is estimated by equating the total void space and total volume of broken rock as shown in Fig.1 (Whittaker *et al.*, 1989).

$$V_{caved} = \frac{Kz\pi D^2}{4}$$
$$V_{space} = 4\left(\frac{1}{2}wm^2\cot\phi\right) + mw^2 + \frac{z\pi D^2}{4} \quad (1)$$
$$\therefore z = \frac{4}{(K-1)\pi D^2}\left[2wm^2\cot\phi + mw^2\right]$$

where, ϕ is angle of repose of broken rocks and K = bulking factor of roof rocks. The parameters w and m are gallery width and mining height, respectively. Eq. (1) suggests that caving height will be higher for narrow gallery width than the wider one. If the depth of coal seam (H) is lower than the height of collapsed chimney, a sinkhole appears on the surface. In this case, a cylindrical or conical shape depression occurs on the surface. Ground depression is termed as the depth of top portion of broken rocks in the sinkhole measured from the surface. Theoretically, the depth of this cylindrical depression from the surface can be estimated by equating excess void volume on the surface as shown in Fig. 2 and given in Eq. (2):

$$d = \frac{4\left(2wm^2\cot\phi + mw^2\right)}{\pi D^2} - H(K-1) \quad (2)$$

Ground depression is represented by a positive or negative value of d only if $z \geq H$. A positive value represents ground depression below the surface level. A negative d value signifies that the sinkhole has reached on the surface and void space is completely filled by broken rocks. The value of d will be null if $z<H$.

Since finite element models are developed in two dimension, it has become necessary to estimate z and d for two dimensional space. Theoretical formulation for two dimensional collapsed chimneys is assumed to be rectangular in shape. As before, the similar concept is applied while estimating the caving height and ground depression. However, in order to estimate the area occupied by the galleries in three dimension, following assumptions are adopted.

From earlier analysis it is found that the volume occupied by the caved rocks in the adjoining rooms of a 4-way junction ($2\,wm^2\cot\phi$) is significant as compared to volume of the junction itself (wm^2) and ratio of these two volumes is

$$r = \frac{2m\cot\phi}{w} \quad (3)$$

Assuming similar area ratio in two dimensional analyses, the total void area can be estimated as shown in Fig. 3.

$$A_{space} = mw[1+r] + A_p = mw\left[1 + \frac{2m\cot\phi}{w}\right] + zD \quad (4)$$

where A_p is the area released by the broken rocks in the roof. Hence equating area of void space and area

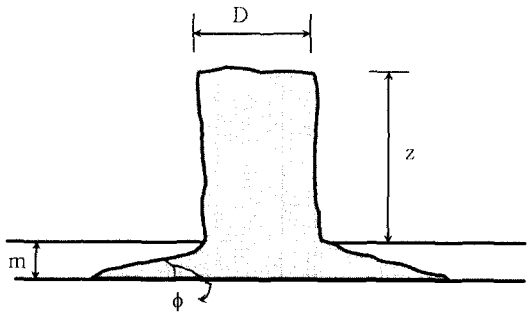

Fig. 1. Caved rocks filled collapsed chimney

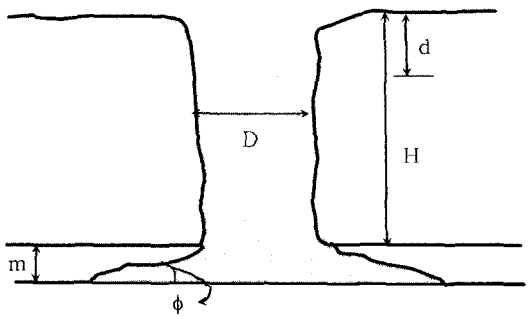

Fig. 2. Depth of ground depression for $z > H$

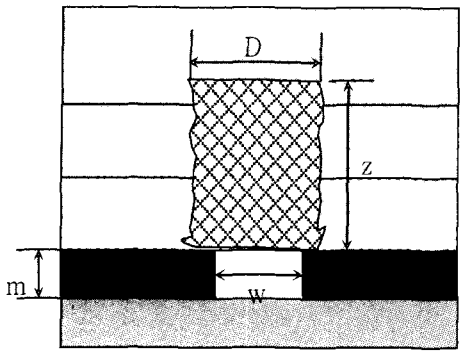

Fig. 3. Two dimensional approximation of sinkhole formation

occupied by the broken rocks, the height of cavity will be,

$$z = \frac{mw + 2m^2 \cot\phi}{D(K-1)} \tag{5}$$

As before, if the collapsed chimney reaches to the surface, a vertical ground depression is developed and it is estimated as

$$d = \left[\frac{mw + 2m^2 \cot\phi}{D}\right] - H(K-1) \tag{6}$$

3. Concept of active-passive-active finite element

As mentioned before, a special finite element is developed for simulating cavity formation in the roof and analyzing the goaf region. This element is termed as "Active-Passive-Active" element by authors. An active element in the model represents a solid finite element formulated with elastic-plastic material behavior. A passive element, however, represents an excavated area or void area generated due to rock fall. The major idea of making a passive element is to generate void area in the roof once the element fails due to tension. This way, roof element is eliminated from the model and thus void area can extend upward in the same fashion as collapsed chimney or sinkhole is formed. The characteristics of passive element are same as an active solid element in the model except this element is not included in the formulation of global stiffness matrix and load/reaction force vectors (Fig. 4). In this figure, the gray or excavated area will be modeled with passive elements and other portion of the model will be composed of active solid elements. If any node in the excavated area is surrounded by passive elements, that node is considered as "passive node" and all degrees of freedom are constrained as shown in the Fig. 4. Similarly, if any node occurring in the collapsing region is surrounded by passive elements, that node will be declared passive and displacements will be constrained for further iterations.

Thus for a passive node the displacement in x- and y- directions are restrained as

$$\begin{Bmatrix} u \\ v \end{Bmatrix}_{pn} = \{0\} \tag{7}$$

The stiffness matrix for a passive element is NULL and does not contribute to the global stiffness matrix formulation. Thus the components of stiffness matrix

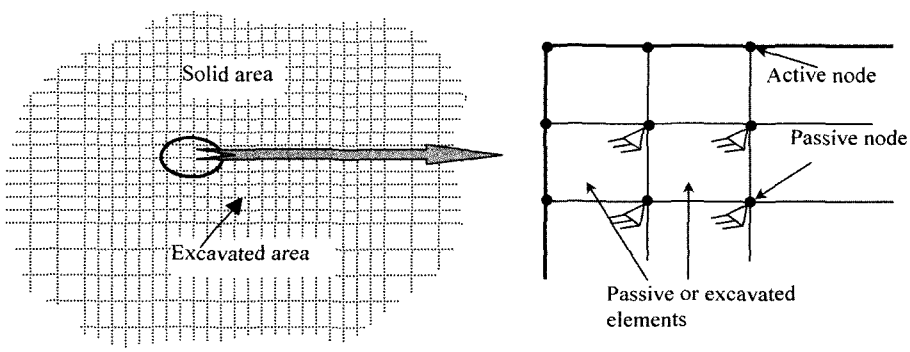

Fig. 4. Concept of passive element and passive node

and also the load vector of a passive element are

$$[K]_{pe} = [\mathbf{0}] \quad \text{and} \quad \{F\}_{pe} = \{\mathbf{0}\} \tag{8}$$

A passive element can be made active at any iteration of a load step with a set of specified material properties. Once a passive element becomes active, it behaves as solid element in the model. If any passive node is attached to that element, that node will be made active at that time. In the same way, an active element can also be made passive at any iteration of a load step depending on the stress conditions or any user-defined criteria. Thus an element in the roof above the excavated area is initially "Active" and then it may become "Passive" to simulate cavity area and once certain conditions are satisfied it can be made "Active" again as a goaf element.

3.1 Plastic correction for active elements

Plastic correction of active elements (other than goaf elements) is applied based on generalized Hoek and Brown failure criterion as given in the following equation.

$$\sigma_1 = \sigma_3 + \sigma_c\left(m_b\frac{\sigma_3}{\sigma_c} + s\right)^a \tag{9}$$

where σ_1 and σ_3 are the principal stresses and should be arranged as $\sigma_1 \le \sigma_2 \le \sigma_3$(considering compressive stress is negative). Principle stresses and their direction cosines are obtained from Cartesian stress vector recognizing σ_z as one of the principle stresses. σ_c is uniaxial compressive strength of intact rock and negative value will be considered. m_b is reduced material constant based on intact property of rock, m_i and Geological Strength Index (GSI) and s and a are rock mass properties based on GSI as given below (Hoek *et al.*, 2002).

$$m_b = m_i \exp\left[(GSI - 100)/28\right],$$
$$s = \exp\left[(GSI - 100)/9\right],$$
$$a = \frac{1}{2} + \frac{1}{6}\left[\left(\exp(-GSI/15) - \exp(-20/3)\right)\right]$$

Fig. 5 shows four different zones viz. compression yield region, tensile yield region, safe region and infeasible region in $\sigma_3 - \sigma_1$ plane. The compressive yield region is designated where Hoek and Brown yield criterion has been violated while tensile yield zone is assumed where confining stress exceeds user-defined or the maximum tensile strength of rock mass. The safe region implies the stress point in $\sigma_3 - \sigma_1$ plane where both tensile and compressive yield criteria are not satisfied. The infeasible region signifies σ_1 that cannot exceed σ_3 or the value of cannot be lower than the value of σ_1.

Shear yield criterion is applied using Eq. (10) with non-associative flow rule. In this study, Mohr-Coulomb form of plastic potential function is adopted with constant parameter, N_Ψ for deriving plastic corrections with Hoek and Brown yield criterion.

$$g^S = \sigma_1 - \sigma_3 N_\Psi \tag{10}$$

where $N_\Psi = \tan^2(\Psi/2 + \pi/4)$ and Ψ = dilation angle.

Tensile yield criterion is given in Eq. (11) and plastic correction is applied with associative flow rule using plastic potential function given in Eq. (12).

$$f^T = \sigma_t - \sigma_3 = 0 \tag{11}$$

$$g^T = -\sigma_3 \tag{12}$$

In this formulation, it is considered that if the value

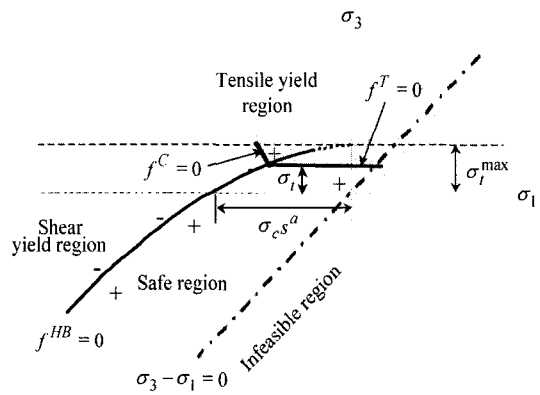

Fig. 5. Different regions in $\sigma_3 - \sigma_1$ plane with Hoek and Brown yield surface

of σ_3 exceeds the maximum tensile strength as estimated using Eq. (13), tensile failure will be declared irrespective of σ_1 value.

$$\sigma_t^{max} = -\frac{s\sigma_c}{m} \tag{13}$$

A composite yield criterion is also developed to demark between shear and tensile yield regions by bisecting the tangent at point C as shown in Fig. 6. The equation of composite yield criterion is given in Eq. (14).

$$f^C = \sigma_3 - \sigma_t + l_p(\sigma_1 - n_p) = 0 \tag{14}$$

where

$$l_p = \sqrt{1+P^2} + P$$
$$K = 1 + am_b(m_b\sigma_t/\sigma_c + s)^{a-1}$$
$$n_p = \sigma_t + \sigma_c(m_b\sigma_t/\sigma_c + s)^a$$

For shear yielding case, plastic strain increments are obtained using Eq. (15) as given below:

$$\Delta\varepsilon_i^p = \lambda^S \frac{\partial g^S}{\partial \sigma_i} \quad i = 1, 3 \tag{15}$$

where λ^S is plastic multiplier and has to be determined

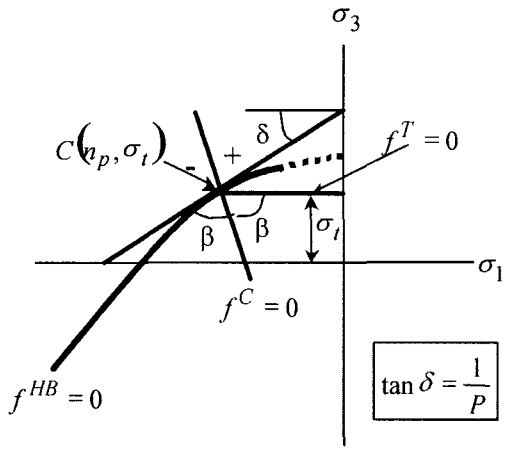

Fig. 6. Composite yield criterion for Hoek and Brown material model

for new stresses that lie on the yield surface. Considering the total strain increment can be divided into elastic and plastic strain increments and stress increment can only be occur due to change in elastic strain increment, new state of stress can be written as (note that all symbols are kept the same as given in Theory and Background manual of FLAC2D software):

$$\sigma_1^N = \sigma_1^I - \lambda^S(\alpha_1 - \alpha_2 N_\psi)$$
$$\sigma_2^N = \sigma_2^I - \lambda^S\alpha_2(1 - N_\psi)$$
$$\sigma_3^N = \sigma_3^I - \lambda^S(-\alpha_1 N_\psi + \alpha_2) \tag{16}$$

where $\alpha_1 = K + 4/3G$ and $\alpha_2 = K - 2/3G$. The parameters K and G are bulk and shear modulus of the material. The stresses expressed by $\sigma_i^I (i = 1, 3)$ are trial stresses obtained from total stress increment prior to plastic correction. For tensile failure case, the flow rule is obtained from Equation 11 with plastic multiplier λ^T.

$$\Delta\varepsilon_i^p = \lambda^T \frac{\partial g^T}{\partial \sigma_i} \tag{17}$$

With the same reasoning as given above, the new state of stress can be obtained as

$$\sigma_1^N = \sigma_1^I + \lambda^T\alpha_2$$
$$\sigma_2^N = \sigma_2^I + \lambda^T\alpha_2$$
$$\sigma_3^N = \sigma_3^I + \lambda^T\alpha_1 \tag{18}$$

The plastic multipliers are obtained by solving following equations directly for λ^T and using Newton-Rapson procedure for λ^S:

$$\lambda^T = \frac{f^T(\sigma_3^I)}{\alpha_1} \tag{19}$$

$$\sigma_1^N - \sigma_3^N - \left[m_b\sigma_3^N/\sigma_c + s\right] = 0 \quad \text{or}$$
$$\sigma_1^I - \sigma_3^I + \lambda^S(1 + N_\psi)(\alpha_2 - \alpha_1)$$
$$-\sigma_c\left[m_b(\sigma_3^I - \lambda^S(\alpha_2 - \alpha_1 N_\psi))/\sigma_c + s\right] = 0 \tag{20}$$

After solving λ^S and λ^T, new principle stress can be obtained using Eq. (16) and Eq. (18), respectively. If the trail stress falls inside the safe region, no plastic correction is applied and new principle stresses

are updated with trail stresses. Assuming the direction of principle stresses would not change due to plastic corrections, stresses at Cartesian coordinate system can be obtained using the direction cosines obtained earlier.

4. Validation of finite element method with passive elements

A quarter of circular opening with 4 m diameter is modeled i) with passive elements in the excavation area ii) without passive elements as shown in the Fig. 7. The elastic modulus and Poisson's ratio of rock are assumed to be 20 GPa and 0.25, respectively. Far field stress is assumed to be hydrostatic having magnitude of 2 MPa. Eight nodded quadrilateral elements are used to model the rock mass and passive elements are modeled with 3-noded triangular elements. Linear static analysis is performed for both cases. Fig. 8 shows the axial displacements and Fig. 9 depicts tangential and radial stresses with and without passive elements in the excavation zone. Analytical or closed form solutions are also plotted to compare the results from finite element analysis. It is clear that results obtained using passive elements in the excavation zone are identical to the results of finite element model without them. This proves that the inclusion of passive elements in the excavation area does not alter finite element procedure and can be used effectively to simulate excavation/cavity area created by roof fall.

5. Finite element modeling of sinkhole formation

5.1 Model description and parameters

A single gallery and two pillars model is developed with symmetrical axis lying along the mid vertical line of the gallery. The dip angle of the rock strata is assumed to be zero. One main floor, pillar, roof and top soil are modeled as shown in Fig. 10. The model is constrained horizontally in the vertical planes and vertically in the bottom horizontal plane. Four parameters, width of gallery (w), depth of overburden (D), roof condition (index) (R), and bulking factor (K) are varied to generate sixteen models. Roof index, R is defined to quantify roof conditions based on geological strength index (GSI), compressive strength of intact rock and thickness of the rock strata as given below:

$$R = \frac{\sum_{i=1}^{N}\left(\sigma_{cm}^{i} \times t_i\right)}{\sum_{i=1}^{N} t_i} \tag{21}$$

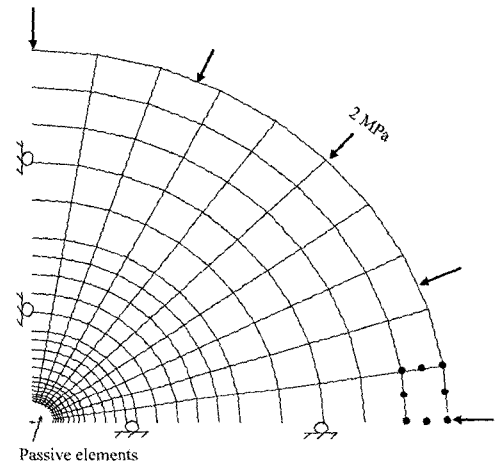

Fig. 7. Finite element mesh of quarter circular opening

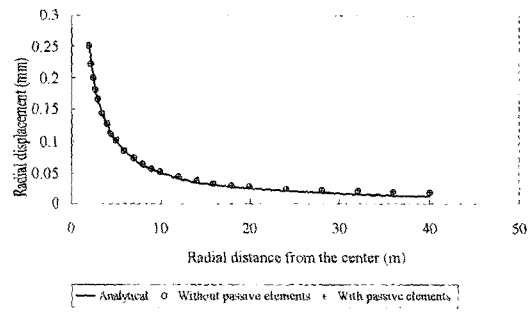

Fig. 8. Radial displacement with radial distance

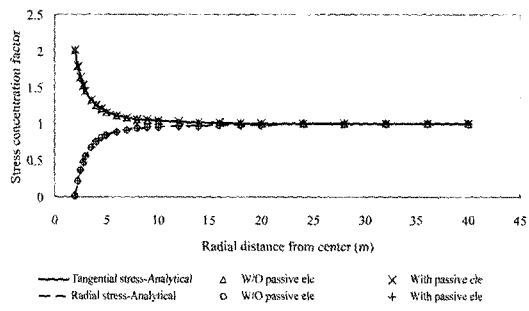

Fig. 9. Tangential and radial stresses with radial distance

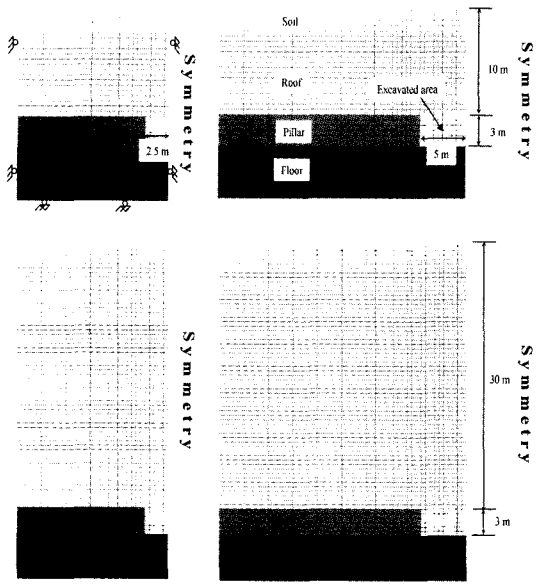

Fig. 10. Dimension of different finite element models

where, σ_{cm}^{i}= rock mass strength of the i^{th} roof strata
$= \sigma_{ci}^{i}(s)^{a}$,
t_i = thickness of the roof strata,
N = number of rock strata above the worked seam

The parameter, ***R*** is a rough measure of competency of the roof. Higher rock mass strength signifies competent rock mass and causes higher value of ***R***. Table 1 provides rock mass properties used in finite element models. It shows that ***R*** value of 0.344 and 6.421 signifies weak and strong roof, respectively. Angle of repose is assumed to be 45 degrees for all models. Rock mass property of pillar indicates weathered limestone strata having *GSI* of 40 and compressive strength of 30 MPa.

Initially, rock mass is analyzed with elastic-plastic material with generalized Hoek and Brown yield criterion as mentioned above. For each load step, several iterations are performed until the force convergence criterion is satisfied. For each sampling point of every element rock mass failure criteria are checked including criterion for sinkhole formation as given in Fig. 11. Once the sinkhole formation process is completed only generalized Hoek and Brown failure criterion are applied to rock mass that reside outside the developed sinkhole zone. Goaf elements are treated linearly. Studies in the past revealed that for longwall mining condition the in-situ stress is usually achieved at a distance of 1/3rd of the mining depth from the faceline (Pappas & Mark, 1993). To account for compaction of goaf, low elastic modulus is assumed for linear stress-strain behaviour of goaf elements.

5.2 Assumptions on modeling sinkhole development process

1. An element occurring in a specified region will be declared "passive" if stress condition at any sampling point of that element during any iteration satisfies tensile yield criterion, i.e.

$$F_t = \sigma_t - \sigma_3 < 0$$

where σ_t = tensile strength of rock mass,
σ_3 = minor principal stress

2. The growth of collapsed chimney is restricted by a radius of ***w***/2 centered at the mid-vertical line of the gallery of width ***w***. Thus, the maximum width (***D***) of the collapsed chimney will be ***w***.
3. Development of sinkhole is considered complete if either of the two conditions is satisfied.
i) Volume of void space and volume occupied by

Table 1. Material properties used in finite element models

Rock Layers	Elastic Modulus (Gpa)	Poisson's Ratio	Density (kg/m^3)	GSI	m_i	σ_{ci}	σ_t (MPa)	Dilation Angle (deg.)	Rock mass strength, σ_{cm}(MPa)
Floor	6.00	0.20	2300.0	60.0	15.0	40.0	4.0	10.0	4.280
Pilar rock	4.00	0.30	2300.0	40.0	10.0	30.0	3.0	8.0	0.992
Roof (weak)	6.00	0.25	2400.0	30.0	7.0	20.0	2.0	6.0	0.344
Roof (strong)	6.00	0.25	2400.0	60.0	20.0	60.0	8.0	10.0	6.421
Roof (soil)	0.10	0.35	2000.0	40.0	7.0	0.5	0.1	5.0	0.017
Gob Material	0.05	0.35	1800.0	-	-	-	-	-	-

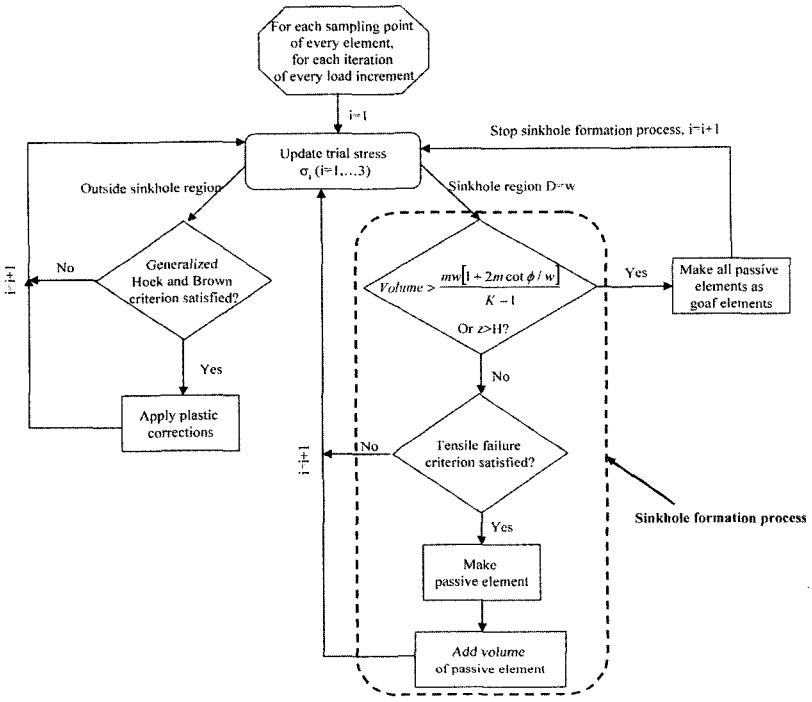

Fig. 11. Sinkhole formation algorithm in FEM

broken rocks is equal as given in the Eq. (4).

ii) If the caving height reaches to the surface. In this case, ground depression depth, d is estimated using Eq. (6).

Once either of these two conditions is satisfied all passive elements below the point of ground depression depth, d including elements in the excavated area will be made active and considered to be broken rocks or goaf elements. The elements residing in the sinkhole development zone and above the ground depression height will remain passive for the rest of the load increments. The stress and displacement vectors for each goaf element are initialized to zero. For subsequent load steps, these elements are included into global stiffness matrix and calculation of load/reaction force vectors. Goaf elements are assumed to be linear-static material and no plastic corrections are applied.

The total void space below the ground depression depth is completely filled with goaf elements. However, in reality, there will be air space in between broken rocks and due to this reason goaf elements are modeled with low stiffness and overall bulk density of goaf area.

5. Time dependent deformation is not considered.

6. Results and discussions

In the following sections, results of finite element analysis are discussed based on caving height, ground depression and stresses on the pillars and goaf region.

6.1 Caving height

Fig. 12 shows the relationship between ratio of caving height to mining height (z/m) with depth of mine and width of gallery when weak strata exits in the roof. It can be seen that sinkhole appears on the surface for shallow depth mine irrespective of gallery size and bulking factor of roof rock. However, for relatively deeper mine (H=30 m) sinkhole occurs on the surface for lower bulking factor and smaller gallery size. For wider gallery size (w=10 m), caving height will reach up to 83% and 37% of the depth of the mine for bulking factor of 1.2 and 1.5, respectively. These results suggest that in the presence of weak strata in the roof, possibility of sinkhole appearance on the surface is

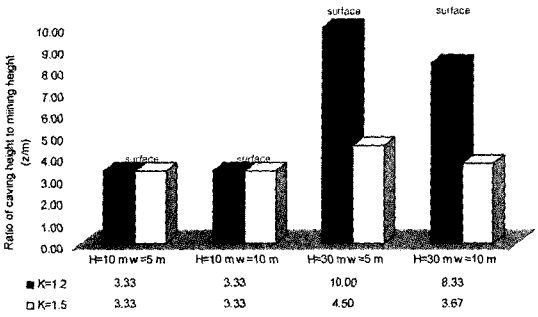

Fig. 12. Height of cavity of collapsed chimney for weak roof condition

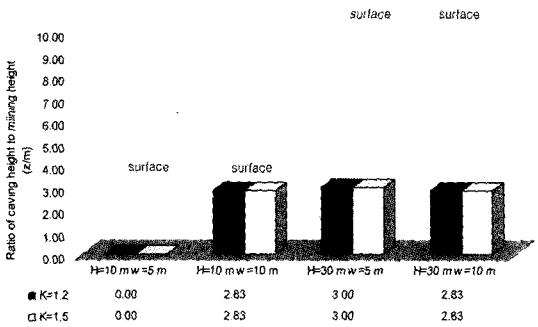

Fig. 13. Height of cavity of collapsed chimney for strong roof condition

higher with smaller gallery size having lower bulking factor of roof rock.

As expected stronger roof strata restrict the sinkhole development process and thus height of cavity does not exceed the depth of cover (Fig. 13). However, for shallow depth mine with wider gallery, caving height may reach up to 94% of the depth causing cracks and fractures on the surface. For relatively deeper mine, caving height will be restricted in the roof itself reaching about 28 to 30% of the depth from the bottom of the mine roof.

6.2 Ground depression

Ground depression (d) is estimated from the finite element results and plotted in Fig. 14 for weak roof condition. As expected ground depression will be higher for lower bulking factor since the volume expansion is less. It is found that ground depression for K=1.2 can be 180% and 100% higher as compared to K=1.5 for gallery width of 5 m and 10 m, respectively. These results signify the importance of bulking factor in determining depth of ground depression. Rocks with higher bulking factor may fill the entire underground void space having low or no ground depression. On the other hand, cavity space created by fallen rocks may not be filled completely due to low volume expansion of broken rocks causing a deeper ground depression.

6.3 Stresses on the pillar and goaf

Vertical stress concentration factor on the top of the pillar is plotted against distance to gallery width ratio based on gallery width and depth of the mine (Fig. 15(a)~(d)). For shallow depth mine having weak roof strata, the peak stress concentration factor on the pillar shows higher value in the presence of wider gallery or excavation area. Since the cavity height has reached to the surface and pillar did not fail the peak stress concentration factor is as high as 2.4 for wider excavated area (Fig. 15(b)). Vertical stress carried by goaf (broken and fallen rocks) is also higher if wider excavation is made since more confining stress will be developed in that region and as a result higher overburden load will be transferred into this area. However, in the presence of stronger roof strata cavity is formed up to 94% of the depth and the goaf region are not yet filled. As a result vertical stress on the pillar is low showing a 41% reduction from the fully grown goaf region. It is also noticed that higher bulking factor causes higher concentration of vertical stress on the pillar due to higher percentage of filling of void space.

Vertical stress concentration for deeper mine suggests

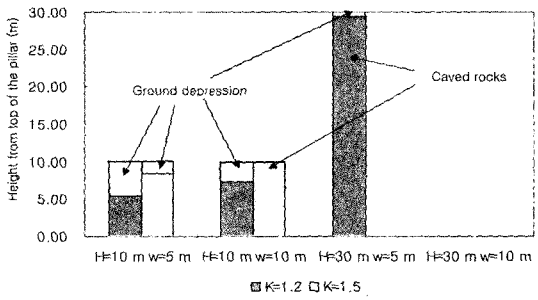

Fig. 14. Ground depression due to sinkhole for weak roof condition

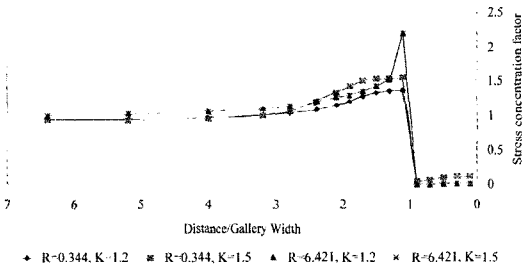

(a) w=5 m, H=10 m

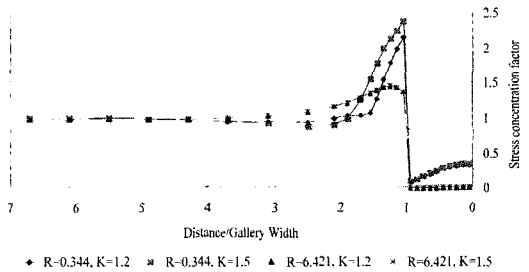

(b) w=5 m, H=10 m

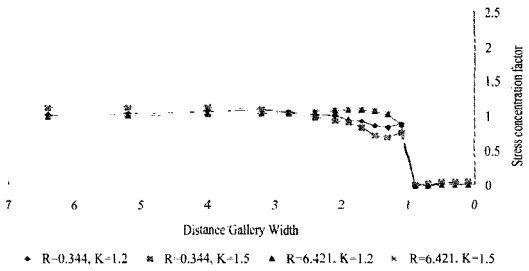

(c) w=5 m, H=30 m

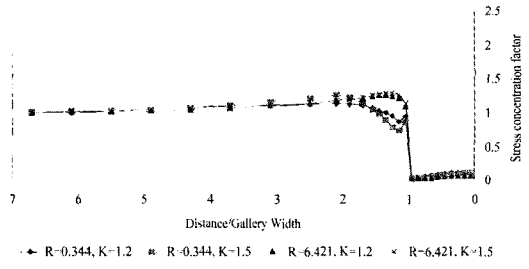

(d) w=10 m, H=30 m

Fig. 15. Vertical stress concentration on top of the pillar

that the pillar has yielded due to additional stress and thus location of peak vertical stress is transferred inside the pillar. The peak vertical stress concentration factor for strong roof condition has decreased by 50% from shallow depth mine. In this case, near the pillar edge (yielded region), vertical stress is lower for higher bulking factor. However, the maximum vertical stress concentration is higher for higher bulking factor as in the case of shallow depth mine.

7. Conclusions

Sinkhole type subsidence causes ground depression on the surface and may also damage properties and surface structures if it occurs in near a populated area. Assessment of sinkhole occurrences is important to provide early warning or generation of subsidence hazard maps.

In this study, a numerical procedure is developed to simulate sinkhole development process using active-passive-active elements. Detailed procedure of this technique is provided in this paper. The study concludes the followings:

- Passive elements can be used in the finite element procedure to simulate excavation area, cavity formation due to roof fall or any other open space that may be created underground
- Possibility of sinkhole occurrences is higher for shallow depth mine with weak roof conditions. However, for deeper mine, possibility of sinkhole occurrences remains significant for shorter gallery size with lower bulking factor of roof rocks
- Existence of strong roof restricts the formation of collapsed chimney for shallow depth mine with shorter gallery size. It is found that in the presence of wider gallery the height caved rocks can be as high as 9.4 m for shallow depth (H=10 m) mine. However, for deeper mine, higher stress conditions may allow roof to collapse even for shorter gallery size. In this study it is found that the height of caved zone can be 28 to 30% of the depth of the mine.
- Bulking factor of roof rocks plays a significant role in determining the depth of ground depression. In general, lower bulking factor increases the chance of higher ground depression as much as 180% as compared to higher bulking factor.
- Finally, the concept of active-passive-active elements will be applied for more complicated ground

conditions having multiple galleries to generate data for the assessment of sinkhole occurrences over underground mines.

Acknowledgements

Financial support was provided by a grant from the office of the Prime Minister of Korea (Basic Research Project).

References

1. Choi S.O. *et al.*, 2004, Development of the Techniques for Reducing the National Disaster caused by Ground Subsidence, 1st year report for project no. M1-0324-00-0013-03-B31-00-005-00, Ministry of Science and Technology of Korea, 232.
2. FLAC 2D, version 4.0: Theory and Background Manual, 2002, Itasca Consulting Group, Inc., Minneapolis, Minnesota, USA.
3. Gray R.E, Bruhn R.W and Turka R.J, 1978, Study and Analysis of Surface Subsidence Over Mined Pittsburgh Coalbed, Final Report, Formally US Bureau of Mines, Contract J0366047, NTIS PB 281 511, 362.
4. Hoek E., Torres C.C., and Corkum B., 2002, Hoek and Brown Failure Criterion - 2002 Edition, 5th North American Rock Mechanics Symposium and 17th Tunneling Association of Canada Conference (NARMS-TAC), 267-271.
5. KIGAM report, 1993, Study on the stability diagnosis and evaluation for the Boopyung mine area, 284.
6. Kratzsch H, 1985, Mining Subsidence Engineering, Springer-Verlog Publication, 543 (translated by R.F.S. Fleming).
7. Najjar Y. and Zaman M., 1993, Numerical Modeling of Ground Subsidence Due to Mining, Int. J. Rock Mech. Min. Sci. & Geomech. Abstr., 30.7, 1445-1448.
8. Pappas, D.M. and Mark, C, 1993, Behavior of Simulated Longwall Gob Material, Report of Investigations, USBM, US department of interior, RI-9458.
9. Peng S.S., 1992, Surface Subsidence Engineering, SME Publication, pp.161.
10. Whittaker B.N and Reddish D.J, 1989, Subsidence Occurrence Prediction and Control, Elsevier Publication, 528.

Debasis Deb

1990년 Dept. of Mining Eng., IIT(Indian Institute of Technology, Kharagpur), BS
1994년 Dept. of Mineral Eng., Univ. of Alabama, MS
1997년 Interdisciplinary Ph.D of Dept. Mineral Eng. & Dept. of Engineering Mechanics, Univ. of Alabama, Ph.D
Tel: 042-868-3224
E-mail: deb@kis.kigam.re.kr
현재 IIT 교수/ 한국지질자원연구원 지반안전연구부 Postdoctoral Research Fellow

신 희 순

1976년 서울대학교 공과대학 자원공학과 공학사
1978년 서울대학교 대학원 자원공학과 공학석사
1986년 서울대학교 대학원 자원공학과 공학박사
Tel: 042-868-3014
E-mail: shinhs@kigam.re.kr
현재 한국지질자원연구원 지반안전연구부장 책임연구원

최 성 웅

1987년 서울대학교 공과대학 자원공학과 공학사
1989년 서울대학교 대학원 자원공학과 공학석사
1994년 서울대학교 대학원 자원공학과 공학박사

Tel: 042-868-3243
E-mail: choiso@kigam.re.kr
현재 한국지질자원연구원 지반안전연구부 선임연구원